

---

# TOWARDS SUPERIOR QUANTIZATION ACCURACY: A LAYER-SENSITIVE APPROACH

---

Feng Zhang , Yanbin Liu , Weihua Li , Jie Lv , Xiaodan Wang , Quan Bai 

## ABSTRACT

Large Vision and Language Models have exhibited remarkable human-like intelligence in tasks such as natural language comprehension, problem-solving, logical reasoning, and knowledge retrieval. However, training and serving these models require substantial computational resources, posing a significant barrier to their widespread application and further research. To mitigate this challenge, various model compression techniques have been developed to reduce computational requirements. Nevertheless, existing methods often employ uniform quantization configurations, failing to account for the varying difficulties across different layers in quantizing large neural network models. This paper tackles this issue by leveraging layer-sensitivity features, such as activation sensitivity and weight distribution Kurtosis, to identify layers that are challenging to quantize accurately and allocate additional memory budget. The proposed methods, named SensiBoost and KurtBoost, respectively, demonstrate notable improvement in quantization accuracy, achieving up to 9% lower perplexity with only a 2% increase in memory budget on LLaMA models compared to the baseline.

**Keywords** Quantization · Large Language Model · Linear Programming · Transformer · PTQ · LLaMA-2

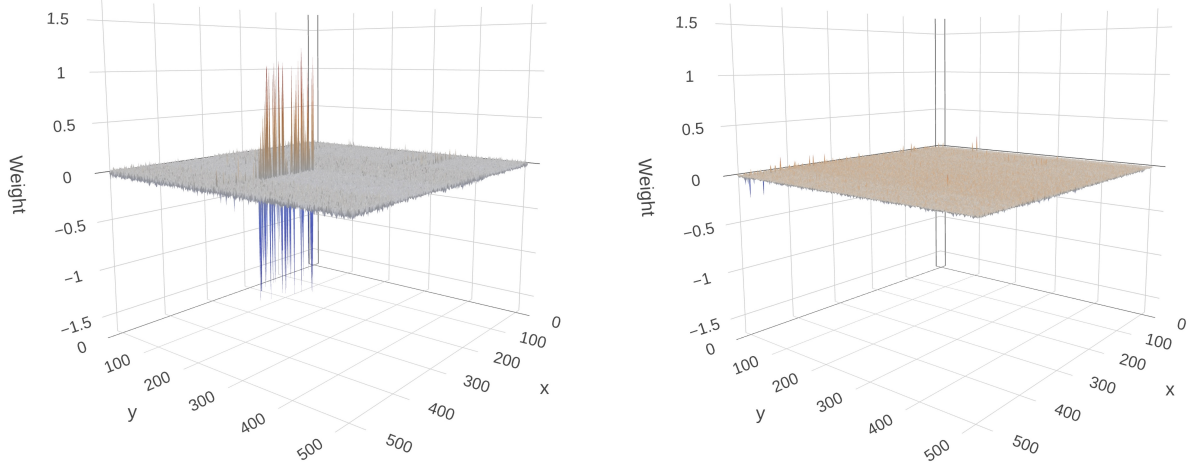
## 1 Introduction

Large Language Models (LLMs) have significantly advanced artificial intelligence, demonstrating human-like capabilities in natural language comprehension, problem-solving, logical reasoning, and knowledge retrieval. These models power a wide range of applications, from chatbots and virtual assistants to code generation and scientific discovery. However, their deployment is hindered by substantial computational and memory demands, which necessitates the needs for efficient model compression and quantization techniques to low the bar of entry.

Quantization techniques aim to reduce the memory footprint and computational requirements of LLMs while preserving their performance. Existing quantization methods, such as AWQ [1], GPTQ [2], BnB [3], and HQQ [4], predominantly employ uniform quantization configurations. While effective to some extent, these approaches fail to consider the varying quantization difficulty across different layers of billion-scale models.

Deep neural network model's weights are typically initialized using the Kaiming [5] or the Xavier initialization method [6], leading to a zero-centered normal distribution with a standard deviation usually less than 1. Outliers are introduced during model training due to several reasons. For example, An et al. [7] revealed that softmax attention is the root cause of outliers in transformer-based neural network models. Additionally, multiple studies [8, 9, 10] discovered that layer normalization contributes to the introduction of outliers. Weights with significant outliers are challenging to quantize accurately since the accommodation of outliers squeezes most normal weights into a narrower range, resulting in an imprecise representation of these weights. The uneven presence of outliers across layers leads to varying quantization difficulty across layers in a particular LLM. As illustrated in Figure 1a and Figure 1b, the weight magnitudes in the `self_attn.o_proj` module differ significantly between the second layer and the last layer. While the last layer shows substantial outliers, the second layer exhibits no notable outliers. This suggests that a uniform quantization approach may not be optimal.

To address this, MXQ [11] introduced a mixed-integer linear programming (MiLP) based approach to assign differentiated quantization configurations while maintaining an overall memory budget. However, despite its adaptive allocation strategy, MXQ-quantized models often underperform compared to the baseline methods such as HQQ, BnB, and AWQ,



(a) This figure demonstrates the subset of the weights (the  $512 \times 512$  sub-region centered at (2533, 3037)) in the second layer of self-attention output projection module of the Llama-2-7B model. The presence of extensive long spikes indicates significant outliers inside the layer of the self attention output projection module.

(b) This figure shows a flat plane of subset of the weights (the  $512 \times 512$  sub-region centered at (2533, 3037)) in the second layer of self-attention output projection module of the Llama-2-7B model.

indicating that the MXQ quantization approach may not effectively prioritize quantization accuracy over memory efficiency in the trade-off.

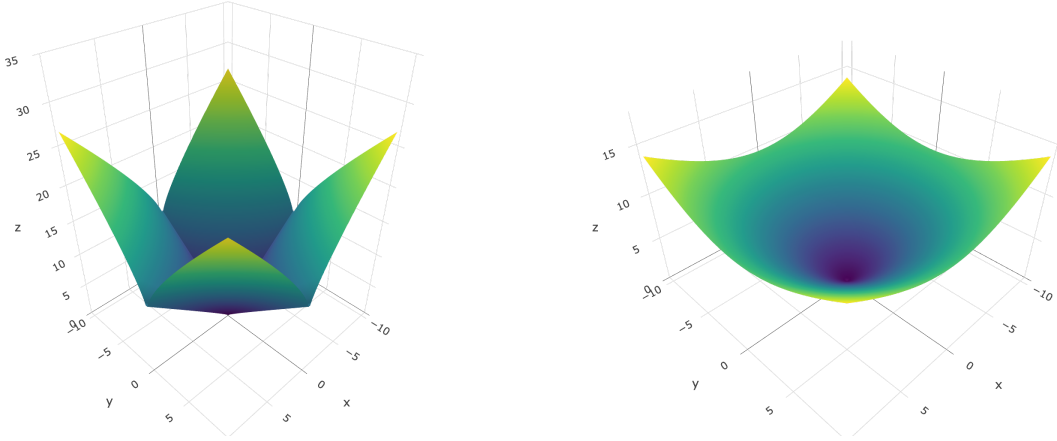
Additionally, prior research [12, 13, 14] has shown that the importance of weights within a deep neural network is non-uniform. Motivated by these observations and the limitations of the state-of-the-art quantization techniques, this paper introduces a novel approach based on layer sensitivity analysis. We hypothesize that memory allocation contributes equally to quantization accuracy across most layers in LLMs, but a subset of layers, termed sensitive layers, require additional memory to maintain optimal performance. Identifying these layers and selectively allocating extra memory resources can enhance overall quantization accuracy with minimal additional cost.

Our proposed method leverages layer-wise sensitivity metrics, including activation sensitivity (hereafter referred to as "sensitivity") and weight distribution kurtosis [15], to identify demanding layers. By selectively allocating additional memory to these layers while slightly relaxing the overall memory constraint, we achieve improved quantization accuracy without incurring significant overhead. Our main contributions are as follows:

- We empirically explored layer-wise activation sensitivity to quantization error on multiple transformer-based LLM families, revealing the robustness of sensitivity within a family of models and their fine-tuned variants.
- We proposed a simple outlier detection algorithm to discover sensitive layers with activation sensitivity scores or Kurtosis metrics.
- Based on the outlier detection algorithm, we proposed the SensiBoost and KurtBoost methods that outperform HQQ with a reduction in perplexity up to 9% while increasing memory budget only by 2%.

## 2 Related Works

The quantization techniques have been extensively studied to address a wide range of use cases, including inference [2, 1], KV cache compression [16], fine-tuning [3, 17] and optimizer state [18]. These techniques can be generally divided into two categories: 1) Quantization Aware Training (QAT) [19], which is tightly coupled with the resource-intensive and time-consuming training process, and 2) Post Training Quantization (PTQ) [20], a training-free method. In this paper, we focus on a specific class of the PTQ method known as weight-only quantization method. Specifically, weight-only quantization can be further categorized into calibration-based and calibration-free methods, depending on whether an additional calibration dataset is adopted during quantization. The following section discusses the weight-only quantization methods.



(a) This figure illustrates the visualization of the two-variable  $L_{p=0.7}$ -norm function as a surface in 3D space. This  $L_p$ -norm is employed by HQQ to preserve outliers in weights of LLMs.

(b) This figure illustrates the visualization of the two-variable  $L_{p=2}$ -norm function as a surface in 3D space.

## 2.1 Calibration-based Methods

The calibration-based approaches leverage the Hessian matrix and Fisher information. While often achieving better quantization accuracy, they tend to be slow and challenging to generalize to models with distinct architectures. The representative state-of-the-art implementations of calibration-based approaches include GPTQ and AWQ.

**GPTQ** [2] is based on Optimal Brain Quantizer (OBQ) [21], which quantized one weight at a time while constantly updating all not-yet-quantized weights to compensate for the error incurred by quantizing a single weight. GPTQ improves OBQ by quantizing weight column-wise to eliminate repeated calculation of the inverse of the Hessian Matrix, thus scaling to larger models with parameters as large as a few hundreds of billions. GPTQ has extensively optimized kernels to accelerate mixed-precision matrix multiplication. Thus, the GPTQ quantized models not only save memory but also run faster.

**AWQ** [1] proposes a quantization method to identify the small fraction of “salient” weights by measuring activation magnitude and pre-scaling the weights with a per-channel factor  $s$  to minimize quantization errors based on the observation that the significance of LLM’s weights is non-uniform. Equation 1 formulates the objective function of AWQ:

$$\begin{aligned}
 s^* &= \underset{s}{\operatorname{argmin}} \mathcal{L}(s) \\
 \mathcal{L}(s) &= \|Q(W \cdot s)(s^{-1} \cdot X) - WX\| \\
 Q(W) &= \Delta \cdot \operatorname{Round}\left(\frac{W}{\Delta}\right) \\
 \Delta &= \frac{\max(|W|)}{2^{n-1}}
 \end{aligned} \tag{1}$$

To tackle the non-differentiability of the loss function in Equation 1, AWQ leverages a simple search space, where  $\alpha$  is confined to the interval  $[0, 1]$ , as defined in Equation 2 to find the optimal scale  $s$ .

$$s = sx^\alpha, \quad \alpha^* = \underset{\alpha}{\operatorname{argmin}} \mathcal{L}(sx^\alpha) \tag{2}$$

This approach unifies the treatment of the salient and non-salient weights, eliminating the need to isolate salient weights into separate storage like sparse matrix, and develop specialised mixed-precision matrix multiplication kernel for fast inference. Besides enabling significant memory reduction, AWQ achieves approximately 3 times inference acceleration compared to the FP16 implementation by Huggingface across a wide range of LLMs.

## 2.2 Calibration-free Methods

**HQQ** [4] leverages quantization parameters zero-point  $z$  and scaling  $s$  to minimize the  $L_{p<1}$ -norm between the original weights  $W$  and their dequantized counterpart as defined in Equation 3.

$$\underset{z,s}{\operatorname{argmin}} \phi(W - Q_{z,s}^{-1}(Q_{z,s}(W))) \quad (3)$$

The incorporation of the  $L_{p<1}$ -norm in the loss function  $\phi()$  enables HQQ to model outliers effectively through a hyper-Laplacian distribution, which captures the long-tailed nature of outliers more accurately than the conventional squared error. Figure 2a illustrates the non-convex nature of  $L_{p=0.7}$ -norm (employed by HQQ) as a 3D surface. Figure 2b shows the 3D plot of the  $L_{p=2}$ -norm, a convex function. The  $L_{p<1}$ -norm makes the loss function  $\phi()$  non-convex. Therefore, HQQ converts the optimization of the non-convex loss function  $\phi()$  formulated in Equation 3 to a new formulation denoted in Equation 4 so that it can leverage the Half-Quadratic solver [22].

$$\underset{z,W_e}{\operatorname{argmin}} \phi(W_e) + \frac{\beta}{2} \left\| W_e - (W - Q_z^{-1}(Q_z(W))) \right\|_2^2 \quad (4)$$

By utilizing alternate optimization, Equation 4 is decomposed into two sub-problems as illustrated in Equation 5.

$$\begin{aligned} W_e^{(t+1)} &\leftarrow \underset{W_e}{\operatorname{argmin}} \phi(W_e) + \frac{\beta^{(t)}}{2} \left\| W_e - (W - Q_z^{-1}(Q_z(W))) \right\|_2^2 (sp_1) \\ z^{(t+1)} &\leftarrow \underset{z}{\operatorname{argmin}} \frac{1}{2} \left\| Q_z^{-1}(Q_z(W)) - (W - W_e^{(t+1)}) \right\|_2^2 (sp_2) \\ \beta^{(t+1)} &\leftarrow k\beta^{(t)} \end{aligned} \quad (5)$$

When  $L_{p<1}$ -norm is the loss function, the solution to the first sub-problem( $sp_1$ ) is the generalized soft-thresholding operator[23] as illustrated in Equation 6.

$$\begin{aligned} W_e^{(t+1)} &\leftarrow \operatorname{shrink}_{l_p}(W - Q_z^{-1}(Q_z(W)), \beta) \\ \operatorname{shrink}_{l_p}(x, \beta) &= \operatorname{sign}(x) \operatorname{relu}\left(|x| - \frac{|x|^{p-1}}{\beta}\right) \end{aligned} \quad (6)$$

The second sub-problem( $sp_2$ ) can be converted to Equation 7. The solution, as presented in Equation 8, is the average over the axis where the quantization grouping is carried out.

$$\begin{aligned} z^{(t+1)} &\leftarrow \underset{z}{\operatorname{argmin}} \frac{1}{2} \left\| z - (W_q^{(t+1)} - \frac{W - W_e^{(t+1)}}{s}) \right\|_2^2 \\ W_q^{(t+1)} &= \operatorname{round}(W/s + z^{(t)}) \end{aligned} \quad (7)$$

$$z^{(t+1)} \leftarrow \left\langle W_q^{(t+1)} - \frac{W - W_e^{(t+1)}}{s} \right\rangle \quad (8)$$

HQQ's sole reliance on the weight without considering the layer activation enables it to generalize to models with diverse underlying architectures. HQQ achieves comparable performance compared to the top quantization methods such as AWQ, GPTQ, and BnB while exhibiting extraordinary quantization speed. Experiments show that HQQ is approximately an order of magnitude faster than the state-of-the-art calibration-based methods such as AWQ and GPTQ. In addition, HQQ offers an abundance of options to further optimize the quantization with a wide range of bits to quantize large neural network models. Available bit choices include 2, 3, 4 and 8. It also allows configurable group size, secondary bit and group size for metadata quantization. Furthermore, by adopting the calibration-free approach, HQQ avoids potential over-fitting to calibration datasets, making it model architecture-agnostic and generalizable to not only diverse transformer-based large language models but also multi-modal models.

**BnB** [3] employs a novel high-precision technique to quantize pre-trained model weights to 4-bit NormalFloat (NF4), which employs the Gaussian distribution exhibited in model weights. The 4-bit NormalFloat datatype represents 16 values ( $q_1, q_2, \dots, q_{16}$ ) in the interval  $[-1, 1]$ . Each weight matrix is chunked into small groups for better quantization

accuracy. Additionally, NF4 employs the double quantization technique to reduce the overhead introduced by the granular grouping scheme, a widely adopted strategy by other state-of-the-art quantization methods.

**MXQ** [3] allocates optimal configurations that minimize the sum of Frobenius norm of the difference between the full-precision weight matrices and their quantized counterparts while maintaining the overall memory consumption within constraints set by a global bit budget per parameter. MXQ can be formulated as a Mixed-Integer Linear Programming [24] problem as denoted in Equation 9:

$$\begin{aligned} & \arg \min_{c_1, c_2, \dots, c_N} \sum_{\substack{i \in \{1, \dots, N\} \\ c_i \in C}} \|W^{(i)} - \hat{W}_{c_i}^{(i)}\|_F \\ \text{s.t. } & \sum_{\substack{i \in \{1, \dots, N\} \\ c_i \in C}} \text{stor}(W^{(i)}, c_i) \leq \beta, \\ \text{where } & \text{stor}(W^{(i)}, c_i) = |W^{(i)}| \cdot \left( b_1 + \frac{2b_2}{g_1} + \frac{32}{g_1 \cdot g_2} \right) \end{aligned} \quad (9)$$

where  $c_i = (b_1, g_1, b_2, g_2)$  denotes the configuration parameters used to quantize the  $i$ th matrix of the LLM,  $b_1$  and  $g_1$  represent the bit width and group size for quantizing weights,  $b_2$  and  $g_2$  indicate the bit width and group size to quantize metadata, such as zero points and scales.  $C$  is the set of 12 possible configurations. Additionally,  $N$  is the number of weight matrices to be quantized,  $W^{(i)}$  and  $\hat{W}^{(i)}$  are the  $i$ th full-precision and quantized weight matrices, respectively. The parameter  $\beta$  denotes the overall memory budget in megabytes. By introducing  $M = |C| \times N$  binary decision variables, Equation 9 is further converted to standard LP formulation [25] so that it can be solved efficiently by off-the-shelf LP solvers such as Gurobi [26] and HiGHS [24].

Except for the relatively new MXQ approach, these methods have been adopted extensively in the industry, demonstrating their practicality and efficacy. Nevertheless, the limitations of these methods are worth discussing. First, quantization methods such as GPTQ and AWQ require curated calibration datasets, making it challenging to generalize these methods to other large neural networks such as vision models, which are trained on a mixture of textual and image data. Given the substantial architectural disparities and diverse choices of training datasets for these multi-modal models, curating compatible calibration datasets is definitely a maintenance headache. Second, calibration-dependent approaches tend to rely on GPUs to perform the quantization as a full inference pass is indispensable to measure the quantization error in terms of activation. This prevents offloading the quantization task to CPUs, which is cheaper and more accessible. Additionally, the quantization speed of calibration dataset-dependent methods like AWQ and GPTQ is relatively slow. For instance, the GPTQ method takes approximately 4 GPU hours to quantize the OPT-175B or BLOOM-176B models [2]. Finally, the first four quantization methods surveyed in this chapter employ uniform quantization configurations across the entire model, which may be sub-optimal to address varying difficulty across diverse layers of billion-scale LLMs.

### 3 Layer-sensitive Quantization

#### 3.1 Activation Sensitivity

Transformer-based large language models are composed of multiple layers or blocks [27]. Each layer consists of the self-attention and Multi-Layer Perceptron (MLP, a.k.a. FFN) sub-layers. Specifically, the Llama family model's self-attention includes weights for K, Q, V, and O projections, known as `k_proj`, `q_proj`, `v_proj`, and `o_proj` respectively. Similarly, the MLP sub-layer is composed of weights referred to as `mlp_proj`, `mlp_down`, and `mlp_gate`. The weights in a large language model are not equally important as revealed by the observation from prior study [1], which claims that preserving a small portion of so-called salient weights can significantly improve the quantization accuracy. These weights correspond to particular channels inside a weight matrix. Motivated by this finding, this paper hypothesizes that there also exist sensitive layers that are more severely affected by weight perturbation than others. Protecting such layers by allocating a larger bit budget will result in an improvement in overall quantization accuracy.

**Activation Sensitivity Score** In this section, we define Activation Sensitivity Score, formulated in Equation 10, as mean squared error between the activations obtained by multiplying the original and quantized weight with the input. This metric quantifies layer-wise sensitivity to perturbation introduced by quantization error of a particular model.

$$s_i = \frac{\|W_i \cdot X - Q^{-1}(Q(W_i)) \cdot X\|_2^2}{|W_i \cdot X|} \quad (10)$$

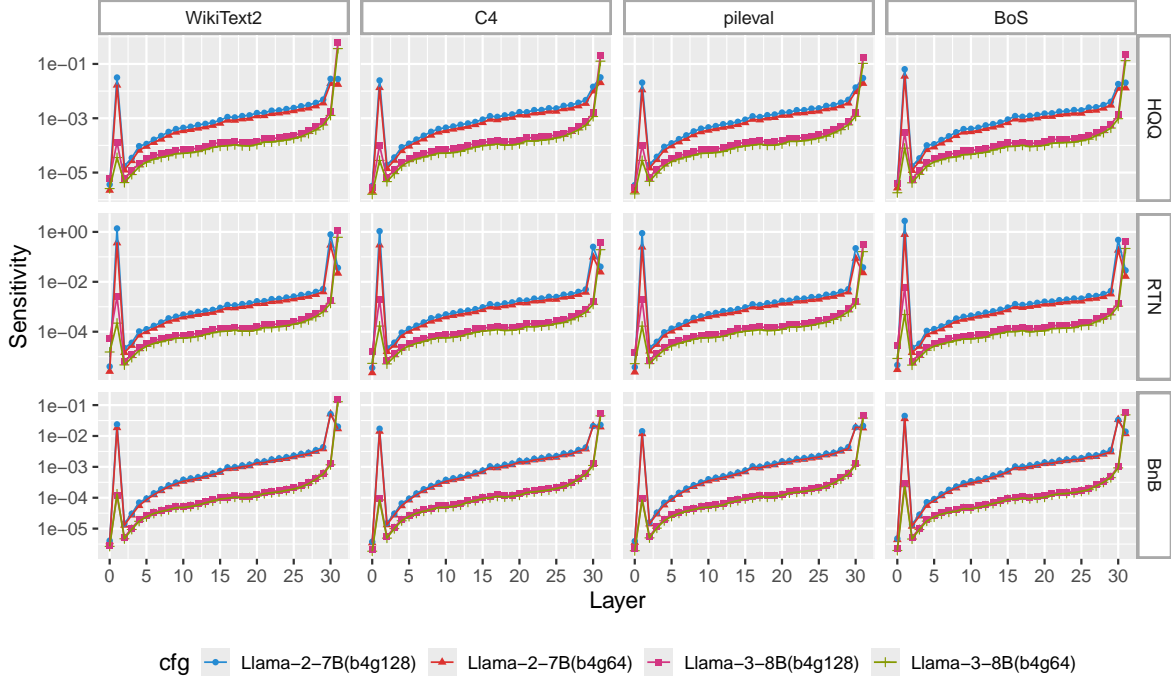


Figure 3: This figure demonstrates the relationship between quantization methods (HQQ, RTN, BnB), datasets (WikiText2, C4 pileval, BoS) and layer-wise sensitivity. The distinct shapes of sensitivity curves for Llama-2-7B and Llama-3-8B models indicate the sensitivity property is model dependent. Meanwhile, the near identical patterns across calibration datasets and quantization methods show that layer-wise sensitivity to quantization error is independent of calibration datasets and quantization methods. For optimal clarity, the figure is best viewed in color and with zoom.

In Equation 10,  $W_i$  denotes the weight in the  $i$ th layer,  $X$  is the input to the model, which is from a small calibration dataset. The  $Q()$  function represents the quantization function to convert the full-precision weight into its quantized counterpart. The  $Q^{-1}()$  function is the inverse of the  $Q()$ .

**Measuring Sensitivity Score** The measurement of sensitivity requires a collection of small calibration datasets, which are fed into the target LLMs layer-by-layer to calculate the output under the full-precision and quantized weights, respectively. Then the mean squared error (MSE) is computed to quantify the sensitivity. Specifically, the three open datasets, WikiText-2, C4 and pileval are utilized to evaluate the robustness of sensitivity. Additionally, a small synthesized dataset named Branch of Science (BoS) is created to further validate if the sensitivity property generalizes to diverse datasets. The BoS is a synthesized dataset composed of a few hundred textual definitions for science, art and business topics such as Mathematics, Physics, Chemistry, Law, Music and Journalism, among others. It is generated using the Llama-2-7B model. The details of the program to produce the BoS dataset are described in Appendix A.3. The BoS dataset is published on Hugging Face under the name schnell18/branch-of-science. The program to measure sensitivity is adapted from the AutoAWQ project on GitHub. For brevity, it is explained in Appendix A.2.

**Sensitivity Properties** The layer-wise sensitivity demonstrates considerable robustness according to the diverse experiments we conducted. We observed that sensitivity is independent of datasets and quantization methods, as evidenced by Figure 3. Moreover, the bit budget only influences the magnitude of sensitivity, not the overall patterns, which remain approximately identical across distinct bit budgets, as presented in Figure 4, where the 3-bit, 4-bit and 8-bit groups share almost the same spikes in layers at the beginning although they are separated by a notable blank. Additionally, fine-tuned models preserve the sensitivity of the base model, which is demonstrated in Figure 5. Finally, experiments on the Llama family model reveal that sensitivity spikes tend to be present at the start and end layers. In summary, the sensitivity properties of large language models can be described as follows:

1. Sensitivity is independent of the dataset and quantization method.
2. Sensitivity pattern is consistent among distinct bit budgets.
3. Fine-tuned models preserve the sensitivity of the base model.
4. Sensitivity spikes tend to be present at the start and end layers.

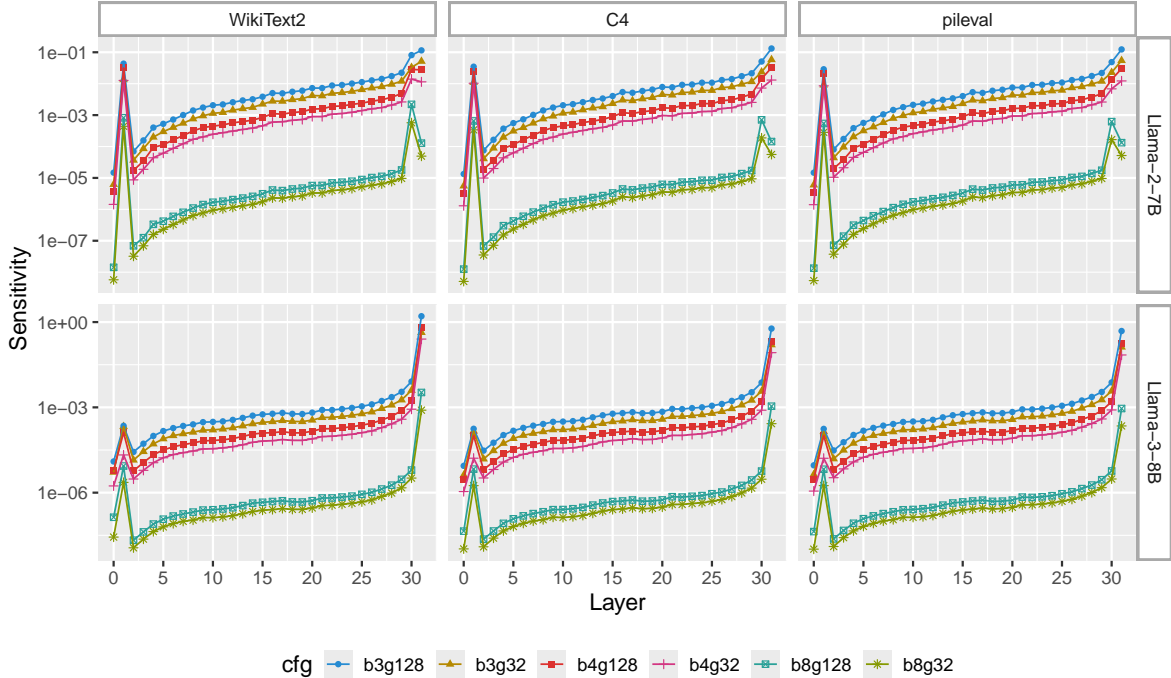


Figure 4: This figure illustrates how bit budget influences layer-wise sensitivity. The magnitude of sensitivity varies among the 3-bit, 4-bit, and 8-bit groups. The 4-bit and 8-bit groups show larger difference as indicated by the wider blank. However, the overall patterns of the three bit groups demonstrate close resemblance. For optimal clarity, the figure is best viewed in color and with zoom.

### 3.2 Kurtosis

The Kurtosis measures the deviation from the normal distribution in terms of tailedness and peakedness [15]. It can be formulated as the standardized fourth population moment about the mean (as denoted in Equation 11).

$$k = \frac{\sum_{i=1}^n (w_i - \bar{W})^4 / n}{(\sum_{i=1}^n (w_i - \bar{W})^2 / n)^2} \quad (11)$$

where  $w_i$  is the  $i$ th weights,  $n$  is the number of weights and  $\bar{W}$  is the mean of the weights. There are three distinct Kurtosis types:

- A value of 3, termed mesokurtic, indicates the perfect conformance to the normal distribution.
- A larger Kurtosis greater than 3, known as leptokurtic, exhibits a narrower peak.
- A lower Kurtosis less than 3, referred to as platykurtic, corresponds to a wider peak and flatter tails.

Existing studies [1, 28] have revealed that preserving outliers is crucial for achieving excellent quantization accuracy. The presence of outliers in a particular layer can be identified using layer-wise Kurtosis metrics make Kurtosis a valuable indicator for determining layers that are challenging to quantify. Layers with the highest Kurtosis values can be isolated using the outlier detection algorithm discussed in the following section.

To measure Kurtosis metrics, the Pearson definition for each quantizable weight matrix is employed to pre-calculate known models by leveraging the `scipy.stats` library [29]. The tool and instructions to generate Kurtosis metrics are described in Appendix A.1. For practical application in the production environment, the Kurtosis metrics could be calculated on the fly since the calculation is relatively lightweight.

### 3.3 Outlier Detection Algorithm

The outlier detection algorithm is designed to single out layers with extreme sensitivity or Kurtosis values so that an additional bit budget can be allocated to improve accuracy. Outliers are usually a small portion of the overall dataset.

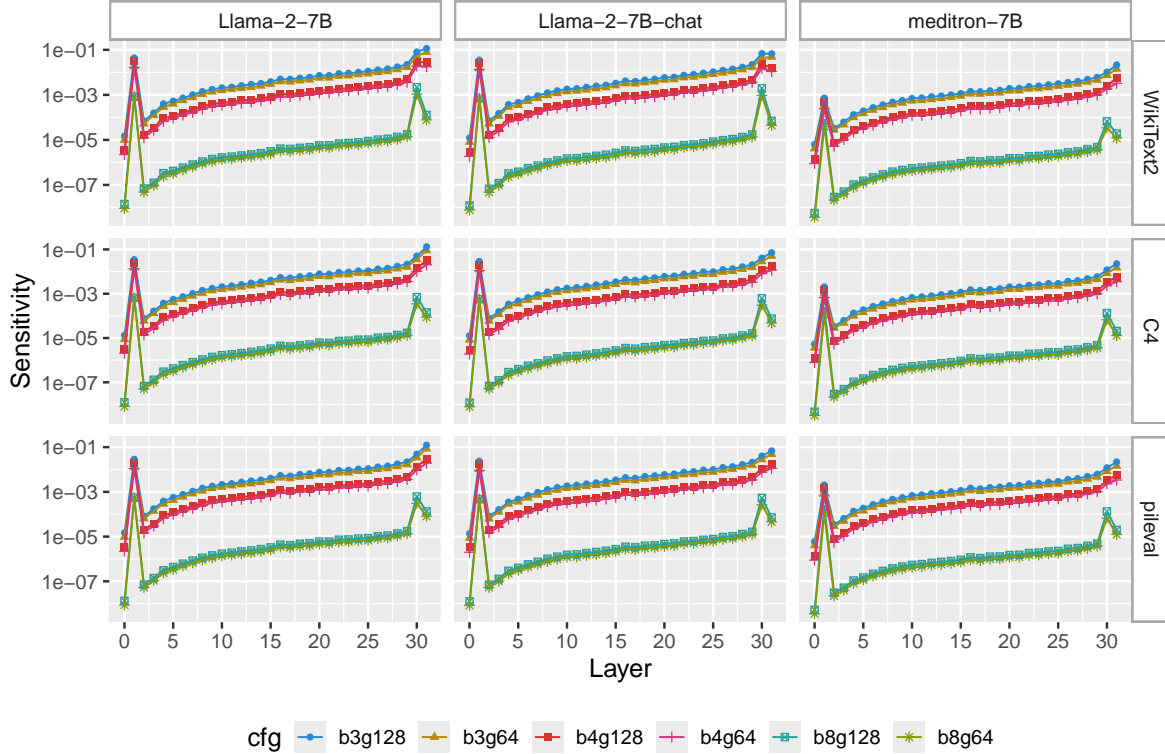


Figure 5: This figure presents the sensitivity patterns among the Llama-2-7B base model and its fine-tuned mutations. Two fine-tuned models are included for comparison. The middle one is Llama-2-7B-chat. And the right is the meditron-7B which is a medical LLM fine-tuned on a carefully curated medical corpus. As indicated by the nearly identical shapes of sensitivity curves, the two fine-tuned models clearly inherit the sensitivity properties from the base model. For optimal clarity, the figure is best viewed in color and with zoom.

The proposed outliers detection algorithm is capable of prioritizing top outliers by rate of change so that only a limited surplus bit budget is allocated. The layer-wise sensitivity or Kurtosis dataset is formulated in Equation 12.

$$S = \{s_1, s_2, \dots, s_n\} \quad (12)$$

The difference between two adjacent layers, denoted as the set  $D$ , is defined in Equation 13 to filter the sensitive data points.

$$D = \{s_2 - s_1, s_3 - s_2, \dots, s_n - s_{n-1}\} \quad (13)$$

For datasets with an approximately ascending pattern, an alternative difference set, as denoted in Equation 14, is defined to use division instead of subtraction, with the advantage of ignoring data points restoring to normal range. This is beneficial in reducing false alarms and economize bit budget.

$$D = \left\{ \frac{s_2}{s_1}, \frac{s_3}{s_2}, \dots, \frac{s_n}{s_{n-1}} \right\} \quad (14)$$

The set  $D$  is assumed to follow the normal distribution. Therefore, the z-score can be leveraged to isolate the outliers. Constrained by memory, only top- $m$  outliers are considered. Equation 15 defines the rule to identify top- $m$  sensitive

layers:

$$\begin{aligned}
Top_m(D') &= \{d \in D' \mid Rank(d, D') \leq m\} \\
D' &= \left\{ d \in D \mid \frac{|d - \mu|}{\sigma} > 3 \right\} \\
\sigma &= \frac{1}{n-1} \cdot \sqrt{\sum_i^n (d_i - \mu)^2} \\
\mu &= \frac{1}{n} \cdot \sum_i^n d_i
\end{aligned} \tag{15}$$

where  $Rank(d, D')$  gives the position of  $d$  when  $D'$  is sorted in descending order. To avoid the influence of extreme values, the mean and standard deviation is calculated using the trimmed approach [30], where the 5% smallest and largest data points are discarded. The actual implementation leverages the `scipy.stats` library. Finally, the sensitive layer can be identified by Equation 16, which adds 1 to the indices returned by Equation 15 since  $|D| = |S| - 1 = n - 1$ .

$$\begin{aligned}
I' &= \{i + 1 \mid i \in ord(x, Top_m(D')) \forall x \in Top_m(D')\} \\
ord(x, S) &= \{i \mid x_i = x, x_i \in S, i \in \{1, 2, \dots, n\}\}
\end{aligned} \tag{16}$$

---

**Algorithm 1** The outlier detection algorithm

---

```

1: Input
2:    $S$    Array of sensitivity scores or kurtosis metrics
3:    $m$    Number of top outliers to return
4:    $t$    Method to construct the difference set
5: Output
6:    $I'$   Array of outlier indices
7: Require  $S = \{s_1, s_2, \dots, s_n\}$ 
8: Ensure  $m \geq 1$ 
9: Ensure  $t == \text{'subtract'}$  or  $t == \text{'divide'}$ 
10: if  $t == \text{'subtract'}$  then
11:    $D \leftarrow \{s_2 - s_1, s_3 - s_2, \dots, s_n - s_{n-1}\}$ 
12: else
13:    $D \leftarrow \left\{ \frac{s_2}{s_1}, \frac{s_3}{s_2}, \dots, \frac{s_n}{s_{n-1}} \right\}$   $\triangleright$  suppress data points restore to normal range
14: end if
15:  $\mu \leftarrow \frac{1}{n} \cdot \sum_i^n d_i$ 
16:  $\sigma \leftarrow \frac{1}{n-1} \cdot \sqrt{\sum_i^n (d_i - \mu)^2}$ 
17:  $i, n \leftarrow 0, |D|$ 
18:  $D' \leftarrow \{\}$ 
19: while  $i \leq n$  do
20:    $z_i \leftarrow \frac{|d_i - \mu|}{\sigma}$ 
21:   if  $z_i > 3$  then
22:      $D' \leftarrow D' \cup \{(d_i, ord(z_i))\}$ 
23:   end if
24: end while
25:  $D'_m \leftarrow sort(D')[: m]$ 
26:  $I' \leftarrow \{\}$ 
27:  $i, n \leftarrow 0, |D'_m|$ 
28: while  $i \leq n$  do
29:    $I' \leftarrow I' \cup \{d'_{m_i}[1] + 1\}$ 
30: end while
31: return  $I'$ 

```

---

Algorithm 1 presents the pseudo-code to locate the outliers, given an array of sensitivity scores or Kurtosis metrics.

### 3.4 SensiBoost and KurtBoost

This section describes SensiBoost and KurtBoost, the two methods leveraging activation sensitivity and Kurtosis metrics to enhance quantization accuracy with a minimal increment in the bit budget. The new approaches are implemented by identifying the sensitive layers using the outlier detection algorithm explained in the previous Section 3.3.

The key steps of the SensiBoost and KurBoost are as follows:

1. Load the pre-calculated sensitivity scores or Kurtosis metrics for the model being quantized.
2. Identify layers for additional allocation using the outlier detection algorithm according to the top- $m$  setting.
3. Allocate normal budget to non-sensitive layers and assign additional budget to sensitive layers according to the boost stop setting.
4. Apply quantization using the underlying quantization method.

Table 1: HQQ bit budgets

stop	budget	$b_1$	$g_1$	$b_2$	$g_2$	stop	budget	$b_1$	$g_1$	$b_2$	$g_2$
0	2.13	2	128	8	128	+1	2.25	2	64	8	128
+2	2.51	2	32	8	128	+3	3.13	3	128	8	128
+4	3.25	3	64	8	128	+5	3.51	3	32	8	128
+6	4.13	4	128	8	128	+7	4.25	4	64	8	128
+8	4.51	4	32	8	128	+9	8.13	8	128	8	128
+10	8.25	8	64	8	128	+11	8.51	8	32	8	128

To apply additional memory allocation, the amount of surplus budget for the sensitive layers can be specified by the number of **boost stops**. When boost stops go beyond the maximum bit budget of the underlying quantization method, the maximum bit budget takes effect. Table 1 presents the 12-stop bit budgets on top of HQQ. For instance, when the base bit budget is 4.13, a setting of 2-stop will quantize the sensitive layers with a bit budget of 4.51. However, when the base bit budget is 8.25, a 2-stop increment request only results in 1 stop, i.e., a bit budget of 8.51.

The number of layers targeted for extra allocation can be restricted based on the descending rank of sensitivity scores or Kurtosis metrics. The resulting layers, referred to as top- $m$  layers, enable further control over the allocation of a limited extra memory budget. Depending on the number of outliers identified, the actual layers eligible for additional allocation might be fewer than the specified value  $m$ . These layers may also vary across modules. No extra memory is assigned to modules without evident outliers. Lastly, when  $m$  is set to 0, all layers identified by the outlier detection algorithm are considered for additional allocation.

### 3.5 Experiments

To assess the effectiveness of the proposed SensiBoost and KurtBoost methods, models quantized using the two approaches were evaluated using the WikiText-2 and C4 datasets to measure the perplexity scores. For each proposed method, various boost stop and top- $m$  configurations were benchmarked. Specifically, these experiments involved benchmarking two boost stop settings (2 and 3) and four top- $m$  values (1, 2, 3, and 0) across three Llama models under six base-bit budget configurations. Furthermore, ablation studies were included to validate the efficacy of the proposed methods. The ablation tests randomly select the layers from a set that explicitly excludes the layers identified by SensiBoost or KurtBoost. To ensure a fair comparison, the amount of extra memory and the layers are identical to those used in SensiBoost or KurtBoost. The complete permutations of the test cases consist of a total of 576 test cases.

The comparisons of the different approaches were made among SensiBoost, KurtBoost, corresponding ablation methods, HQQ, and MXQ, which are presented in Table 2. Win-tie-loss scores were used to qualitatively analyze the proposed methods. These scores were aggregated from the perplexity results benchmarked and paired based on Table 2. Specifically, all perplexity scores were rounded to two decimal places. The perplexity of the primary method (SensiBoost or KurtBoost) was then subtracted from the comparison method to determine the win-tie-loss score. A negative difference awarded the primary method 1 win, a difference of zero awarded 1 tie, and a positive difference awarded 1 loss. Finally, the win-tie-loss scores were aggregated across six quantization configurations, two stop settings, four top- $m$  settings, and two evaluation datasets, providing a summarized win-tie-loss analysis for various method pairs across the three Llama models.

Table 2: Assessment matrix of various approaches

Method	SB	KB	SBAB	KBAB	HQQ	MXQ
SB <sup>1</sup>	-	X	X	-	X	X
KB <sup>2</sup>	-	-	-	X	X	X
SBAB <sup>3</sup>	-	-	-	-	-	-
KBAB <sup>4</sup>	-	-	-	-	-	-
HQQ	-	-	-	-	-	-
MXQ	-	-	-	-	-	-

<sup>1</sup> SB denotes the SensiBoost method.

<sup>2</sup> KB denotes the KurtBoost method.

<sup>3</sup> SBAB denotes the ablation test for SensiBoost method.

<sup>4</sup> KBAB denotes the ablation test for KurtBoost method.

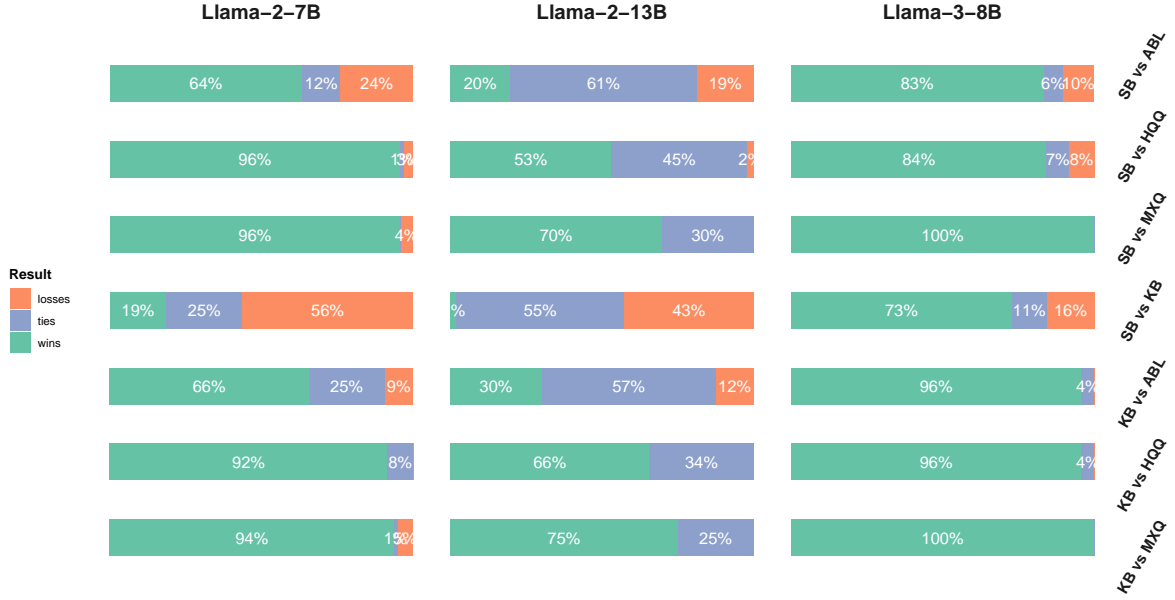


Figure 6: This figure illustrates the win-tie-loss performance of the SensiBoost (denoted as "SB") and KurtBoost (denoted as "KB") methods compared to their ablation test (labeled as "ABL") as well as the baseline methods HQQ and MXQ, across three Llama models. As anticipated, SensiBoost and KurtBoost outperform the baseline methods HQQ and MXQ due to the allocation of additional bit budgets. However, their relatively low win rates (53% against HQQ and 70% against MXQ in the case of SensiBoost, 66% against HQQ and 75% against MXQ for KurtBoost) on the Llama-2-13B model suggest that achieving significant improvements in larger models with a limited extra memory budget is challenging. SensiBoost consistently outperforms its ablation test variant. However, its comparison with the KurtBoost method reveals mixed outcomes: while SensiBoost underperforms on the two Llama-2 models, it demonstrates considerable advantages on the Llama-3-8B model. For optimal clarity, the figure is best viewed in color and with zoom.

### 3.6 Ablation Test

Ablation studies were integrated into the experiments to validate the effectiveness of the proposed SensiBoost and KurtBoost methods, ensuring they outperform random choices. The ablation tests were carried out using random selection and explicitly avoiding choosing layers that could be potentially selected by either SensiBoost or KurtBoost.

Formally, given  $I'$  as defined in Equation 16,  $I'_s$  is the sensitive layers identified by SensiBoost,  $I'_k$  denotes the ones for KurtBoost, the corresponding ablation test layer choices  $J_s$  and  $J_k$  are defined by Equation 17.

$$\begin{aligned}
 J_s &= \{h_1, h_2, \dots, h_p \mid h_i \in \hat{I}, h_i \neq h_j \forall i \neq j, p = |I'_s|\} \\
 J_k &= \{h_1, h_2, \dots, h_q \mid h_i \in \hat{I}, h_i \neq h_j \forall i \neq j, q = |I'_k|\} \\
 \hat{I} &= I \setminus (I'_s \cup I'_k) \\
 I &= \{1, 2, \dots, n\}
 \end{aligned} \tag{17}$$

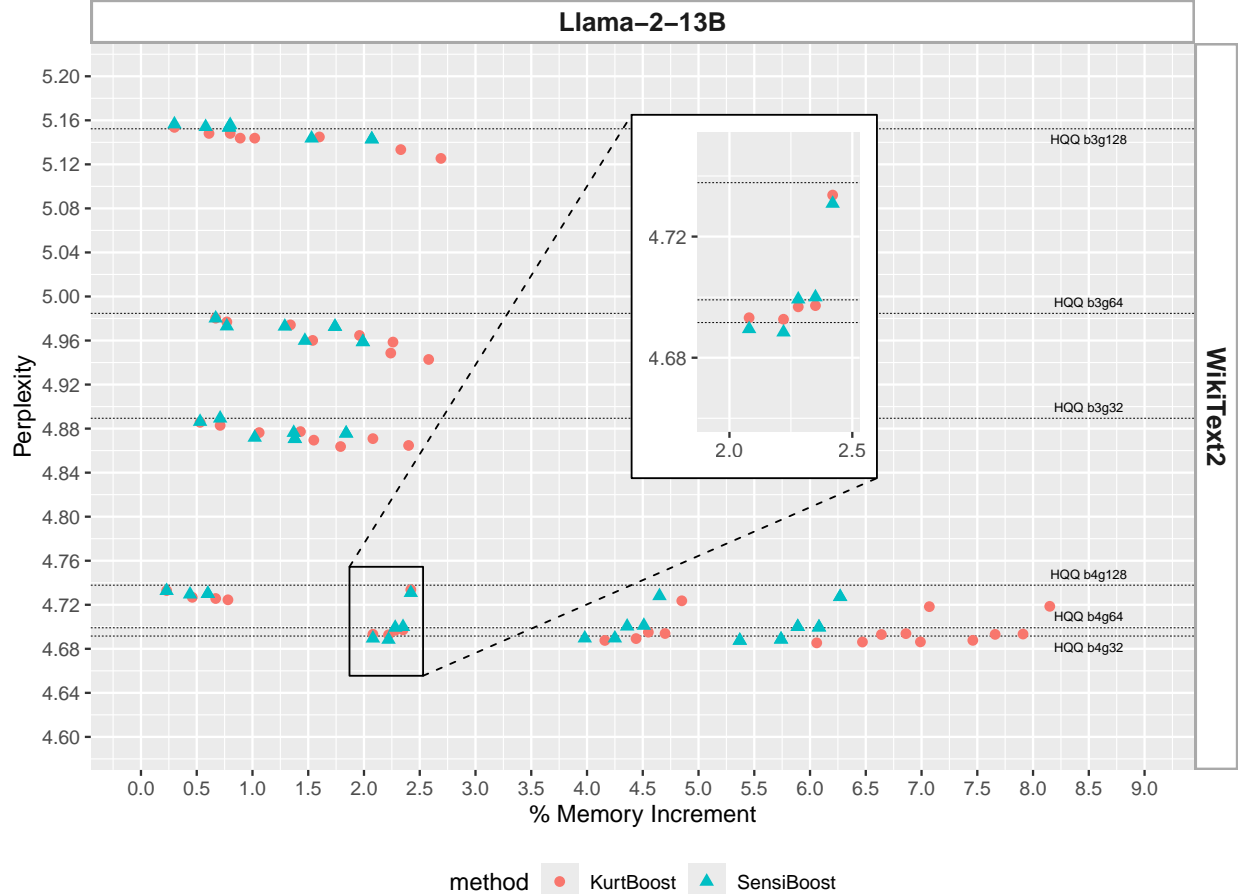


Figure 7: This figure illustrates the perplexity performance of the SensiBoost and KurtBoost approaches evaluated on the Llama-2-13B model using the WikiText2 dataset. The green triangles, representing the SensiBoost method, are positioned closer to the y-axis, indicating that SensiBoost requires less additional memory to achieve comparable performance to KurtBoost. Notably, SensiBoost exhibits a slight advantage over KurtBoost, requiring approximately 2% more bit budget to attain a near-minimal perplexity score, as emphasized in the magnified sub-plot. For optimal interpretation, the figure is best viewed in color and with zoom.

where  $n$  is the number of layers in a particular large language model.

For example, suppose the set  $\{2, 31\}$  represents the sensitive layers discovered by the SensiBoost method, whereas the set  $\{1, 30, 31\}$  is identified by the KurtBoost approach, then the set  $\{3, 28\}$  is a valid choice for ablation test of SensiBoost under  $\text{top-}m = 3$ . Likewise, the  $\{4, 28, 29\}$  is a legitimate ablation test configuration for KurtBoost. However, the set  $\{2, 28, 29\}$  is invalid for ablation test of KurtBoost, since it contains the layer 2 which could potentially enhance quantization accuracy since it is considered as a sensitive layer by the SensiBoost method.

This paper includes two sets of ablation tests designed to validate the efficacy of the SensiBoost and KurtBoost approaches. These tests were conducted under the same configurations as their non-ablation counterparts. Specifically, the configurations consist of two boost stop values and four  $\text{top-}m$  settings, evaluated across three Llama models under six base bit budget configurations.

### 3.7 Results and Analysis

The overall results are presented in this section to qualitatively assess the effectiveness of SensiBoost and KurtBoost by leveraging win-tie-loss comparison. The win-tie-loss diagram, presented in Figure 6, includes the comparisons between the proposed methods (indicated by the row labels) and their ablation variants as well as baselines such as HQQ and MXQ, across three Llama models (denoted by the column labels).

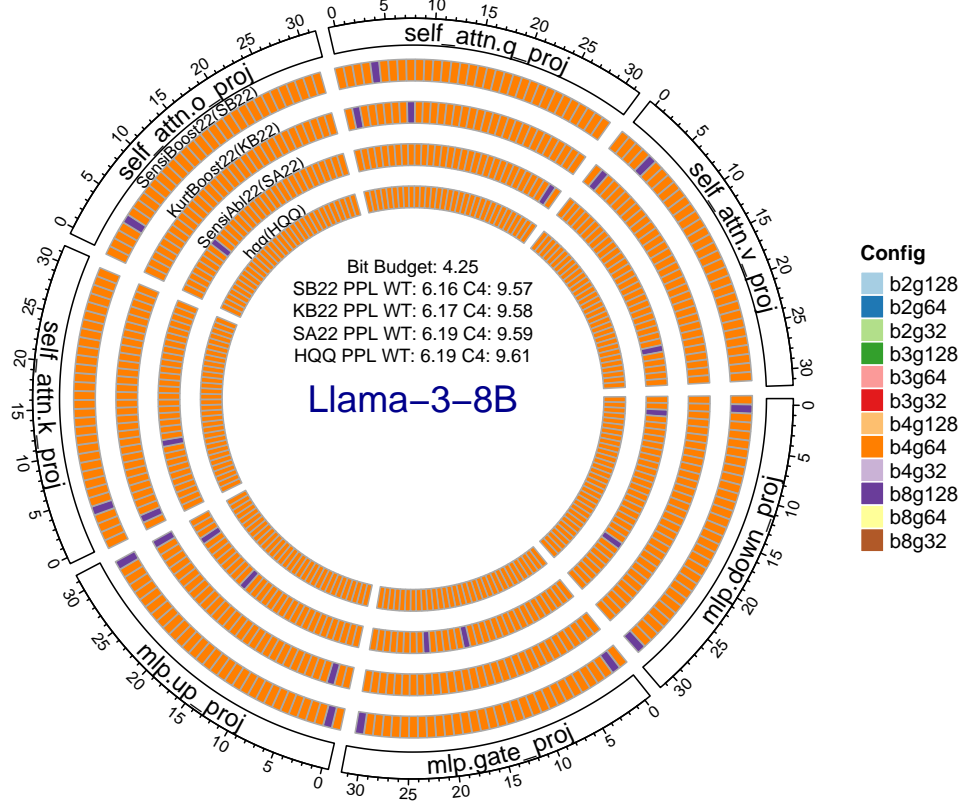


Figure 8: This figure presents a comparison of quantization configuration allocations as determined by SensiBoost, KurtBoost, HQQ and MXQ for the Llama-3-8B model, under a bit budget of 4.25. The colored rings represent the assigned quantization configurations denoted as b2g128 through b8g32, while the text in the center indicates the perplexity scores. As demonstrated by this figure the SensiBoost with a boost stop value of 2 and top- $m$  1, as denoted by SB22, yields a perplexity score of 6.16 on WikiText2, 9.57 on C4, outperforming the HQQ baseline, its ablation variant (SA22) and KurtBoost (KB22). For optimal clarity, the figure is best viewed in color and with zoom.

As anticipated, both SensiBoost and KurtBoost outperform the baseline methods HQQ and MXQ due to the allocation of additional bit budgets. However, SensiBoost’s relatively low win rates (53% against HQQ and 70% against MXQ) on the Llama-2-13B model suggests that achieving significant improvements in larger models with a limited extra memory budget is challenging. KurtBoost performs slightly better than SensiBoost on the Llama-2-13B, achieving 66% win rate against HQQ and 75% against MXQ.

In the context of ablation testing, both methods generally outperform their ablation variants. However, the 20% win rate and 61% tie rate on the Llama-2-13B model suggests that SensiBoost struggles to surpass its ablation counterpart when applied to larger models. In contrast, KurtBoost consistently demonstrates a slight advantage over SensiBoost, achieving higher win rates and lower loss rates across all three models.

### 3.8 SensiBoost and KurtBoost Comparison

The previous section provides an overall comparison of the SensiBoost and KurtBoost approaches. A detailed and direct comparison of the two methods is presented in this section to reveal the relative advantages and disadvantages of the two methods under various scenarios.

As indicated by the win-tie-loss result in Figure 6, SensiBoost tends to be less performant than KurtBoost. However, a deeper examination reveals that SensiBoost requires less additional memory to achieve comparable performance to KurtBoost on the Llama2-7B and Llama-2-13B models. As demonstrated in Figure 7, SensiBoost exhibits a slight advantage over KurtBoost in identifying optimal quantization configuration where it requires approximately 2% more

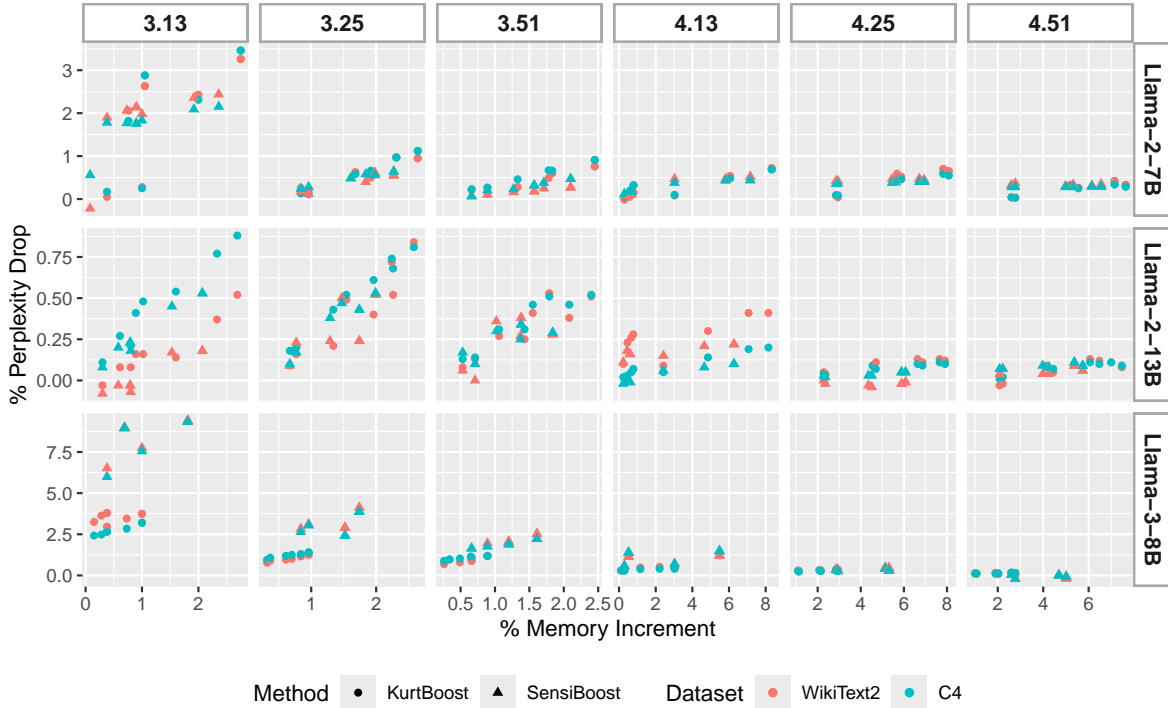


Figure 9: This figure compares the SensiBoost and KurtBoost methods’ performance on quantization accuracy enhancement with additional budget. The X axis denotes the percentage of additional budget assigned. The Y axis represents the percentage of perplexity drop. The improvement is more pronounced around the 3-bit range on the two smaller models Llama-2-7B and Llama-3-8B respectively. Notably, SensiBoost, denoted as triangles, exhibits more aggressive improvement with perplexity drop up to 9% on Llama-3-8B under a budget of 3.13. This figure also demonstrates the challenge of achieving substantial quantization accuracy elevation at higher bit budgets. For optimal clarity, the figure is best viewed in color and with zoom.

bit budget to attain a near-minimal perplexity score, as highlighted in the magnified subplot. This phenomenon replicates to the C4 dataset and the Llama2-7B model.

On the other hand, however, the situation is reversed on the Llama-3-8B model, where KurtBoost is more effective in discovering optimal quantization configuration, which is both memory-efficient and yields better accuracy. The Kurtosis metrics are generated individually for distinct modules in each layer. In contrast, the sensitivity scores are measured by following the neural-network computation sequence, where some modules share the same sensitivity score as they are not standalone computation units. Therefore, the KurtBoost approach may yield more nuanced quantization configurations that are more memory-efficient, as demonstrated in Figure 8, where the `self_attn.o_proj`, `mlp.down_proj`, and `mlp.gate_proj` modules are not assigned extra budget.

In conclusion, both SensiBoost and KurtBoost demonstrate advantages over the baselines and their ablation variants, indicating the effectiveness of the two approaches. Both methods enable model accuracy enhancement by using approximately 2% additional memory budget. Specifically, the improvement is more pronounced in the 3-bit range with perplexity drop up to 9% on Llama-3-8B archived by the SensiBoost as illustrated in Figure 9. This figure also demonstrates the challenge of achieving substantial quantization accuracy improvements at higher bit budgets, as evidenced by the notably flat pattern in the sub-plots for 4.25 and 4.51 configuration.

## 4 Conclusion and Future Work

This paper presents a novel approach to improving quantization accuracy in LLMs by incorporating layer-wise sensitivity analysis. The study empirically explores the impact of quantization errors across multiple transformer-based LLM families, revealing that sensitivity patterns remain consistent within a model family and its fine-tuned variants. This

observation provides valuable insights into the structural characteristics of large-scale neural networks and highlights the need for adaptive quantization strategies.

In the proposed layer-sensitive approach, an outlier detection algorithm is introduced to identify layers that are particularly sensitive to quantization errors. By utilizing activation sensitivity scores and weight distribution Kurtosis metrics, the proposed approach effectively detects layers that require differentiated memory allocation. Building upon these insights, the SensiBoost and KurtBoost methods are developed to selectively allocate additional memory to the most sensitive layers while maintaining an overall memory budget. Experimental results demonstrate that these methods achieve superior quantization accuracy, outperforming the state-of-the-art HQQ approach. Specifically, the proposed techniques lead to a reduction in perplexity of up to 9% while increasing the memory budget by only 2%, striking a balance between efficiency and performance.

The findings of this work suggest that leveraging layer-wise sensitivity features, such as activation sensitivity and Kurtosis, enables more effective quantization strategies with minimal additional computational cost. By integrating these methods into existing quantization frameworks, it becomes possible to enhance the efficiency of LLM deployment without sacrificing model accuracy.

Future research could extend this sensitivity analysis to a broader range of transformer architectures and explore more sophisticated approaches to dynamically adjusting quantization configurations based on computational constraints. As the demand for efficient LLM deployment continues to grow, sensitivity-aware quantization techniques will play a crucial role in optimizing model performance while maintaining practical resource requirements.

## References

- [1] Ji Lin, Jiaming Tang, Haotian Tang, Shang Yang, Xingyu Dang, and Song Han. AWQ: Activation-aware Weight Quantization for LLM Compression and Acceleration. *arXiv preprint arXiv:2306.00978*, 2023.
- [2] Elias Frantar, Saleh Ashkboos, Torsten Hoefer, and Dan Alistarh. GPTQ: Accurate Post-Training Quantization for Generative Pre-trained Transformers, March 2023. *arXiv:2210.17323 [cs]*.
- [3] Tim Dettmers, Artidoro Pagnoni, Ari Holtzman, and Luke Zettlemoyer. QLoRA: Efficient Finetuning of Quantized LLMs, May 2023. *arXiv:2305.14314 [cs]*.
- [4] Hicham Badri and Appu Shaji. Half-quadratic quantization of large machine learning models, November 2023.
- [5] Kaiming He, Xiangyu Zhang, Shaoqing Ren, and Jian Sun. Delving Deep into Rectifiers: Surpassing Human-Level Performance on ImageNet Classification. pages 1026–1034, 2015.
- [6] Xavier Glorot and Yoshua Bengio. Understanding the difficulty of training deep feedforward neural networks. In *Proceedings of the Thirteenth International Conference on Artificial Intelligence and Statistics*, pages 249–256. JMLR Workshop and Conference Proceedings, March 2010. ISSN: 1938-7228.
- [7] Yongqi An, Xu Zhao, Tao Yu, Ming Tang, and Jinqiao Wang. Systematic outliers in large language models. *arXiv preprint arXiv:2502.06415*, 2025.
- [8] Olga Kovaleva, Saurabh Kulshreshtha, Anna Rogers, and Anna Rumshisky. Bert busters: Outlier dimensions that disrupt transformers. *arXiv preprint arXiv:2105.06990*, 2021.
- [9] Xiuying Wei, Yunchen Zhang, Xiangguo Zhang, Ruihao Gong, Shanghang Zhang, Qi Zhang, Fengwei Yu, and Xianglong Liu. Outlier suppression: Pushing the limit of low-bit transformer language models. *Advances in Neural Information Processing Systems*, 35:17402–17414, 2022.
- [10] Nelson Elhage, Robert Lasenby, and Christopher Olah. Privileged bases in the transformer residual stream. *Transformer Circuits Thread*, page 24, 2023.
- [11] F. Zhang, Y. Liu, W. Li, X. Wang, and Q. Bai. A mixed quantization approach for data-free quantization of llms. In *Proceedings of the 17th International Conference on Agents and Artificial Intelligence - Volume 2*, pages 353–363, 2025.
- [12] Mohammad Samragh, Mehrdad Farajtabar, Sachin Mehta, Raviteja Vemulapalli, Fartash Faghri, Devang Naik, Oncel Tuzel, and Mohammad Rastegari. Weight subcloning: direct initialization of transformers using larger pretrained ones. *arXiv preprint arXiv:2312.09299*, 2023.
- [13] Zhiqiu Xu, Yanjie Chen, Kirill Vishniakov, Yida Yin, Zhiqiang Shen, Trevor Darrell, Lingjie Liu, and Zhuang Liu. Initializing models with larger ones. In *The Twelfth International Conference on Learning Representations*, 2023.
- [14] Pavlo Molchanov, Arun Mallya, Stephen Tyree, Iuri Frosio, and Jan Kautz. Importance estimation for neural network pruning. In *Proceedings of the IEEE/CVF conference on computer vision and pattern recognition*, pages 11264–11272, 2019.

[15] Lawrence T. DeCarlo. On the meaning and use of kurtosis. *Psychological Methods*, 2(3):292–307, 1997. Place: US Publisher: American Psychological Association.

[16] Coleman Hooper, Sehoon Kim, Hiva Mohammadzadeh, Michael W Mahoney, Yakun Sophia Shao, Kurt Keutzer, and Amir Gholami. Kvquant: Towards 10 million context length l1m inference with kv cache quantization. *arXiv preprint arXiv:2401.18079*, 2024.

[17] Han Guo, Philip Greengard, Eric P. Xing, and Yoon Kim. LQ-LoRA: Low-rank Plus Quantized Matrix Decomposition for Efficient Language Model Finetuning, January 2024. arXiv:2311.12023 [cs].

[18] Tim Dettmers, Mike Lewis, Sam Shleifer, and Luke Zettlemoyer. 8-bit Optimizers via Block-wise Quantization, June 2022. arXiv:2110.02861 [cs].

[19] Markus Nagel, Marios Fournarakis, Rana Ali Amjad, Yelysei Bondarenko, Mart van Baalen, and Tijmen Blankevoort. A White Paper on Neural Network Quantization, June 2021. arXiv:2106.08295 [cs].

[20] Markus Nagel, Mart van Baalen, Tijmen Blankevoort, and Max Welling. Data-Free Quantization Through Weight Equalization and Bias Correction. pages 1325–1334, 2019.

[21] Elias Frantar and Dan Alistarh. Optimal brain compression: A framework for accurate post-training quantization and pruning. *Advances in Neural Information Processing Systems*, 35:4475–4488, 2022.

[22] D. Geman and G. Reynolds. Constrained restoration and the recovery of discontinuities. *IEEE Transactions on Pattern Analysis and Machine Intelligence*, 14(3):367–383, 1992.

[23] Hicham Badri and Hussein Yahia. A non-local low-rank approach to enforce integrability. *IEEE Transactions on Image Processing*, 25(8):3562–3571, 2016.

[24] Q. Huangfu and J. A. J. Hall. Parallelizing the dual revised simplex method. *Mathematical Programming Computation*, 10(1):119–142, March 2018.

[25] Stephen Boyd and Lieven Vandenberghe. *Convex optimization*. Cambridge university press, 2004.

[26] Gurobi Optimization, LLC. Gurobi Optimizer Reference Manual, 2023.

[27] Ashish Vaswani, Noam Shazeer, Niki Parmar, Jakob Uszkoreit, Llion Jones, Aidan N Gomez, Łukasz Kaiser, and Illia Polosukhin. Attention is All you Need. In *Advances in Neural Information Processing Systems*, volume 30. Curran Associates, Inc., 2017.

[28] Sehoon Kim, Coleman Hooper, Amir Gholami, Zhen Dong, Xiuyu Li, Sheng Shen, Michael W. Mahoney, and Kurt Keutzer. SqueezeLLM: Dense-and-Sparse Quantization. *arXiv preprint arXiv:2306.07629*, 2023.

[29] Pauli Virtanen, Ralf Gommers, Travis E. Oliphant, Matt Haberland, Tyler Reddy, David Cournapeau, Evgeni Burovski, Pearu Peterson, Warren Weckesser, Jonathan Bright, Stéfan J. van der Walt, Matthew Brett, Joshua Wilson, K. Jarrod Millman, Nikolay Mayorov, Andrew R. J. Nelson, Eric Jones, Robert Kern, Eric Larson, C J Carey, İlhan Polat, Yu Feng, Eric W. Moore, Jake VanderPlas, Denis Laxalde, Josef Perktold, Robert Cimrman, Ian Henriksen, E. A. Quintero, Charles R. Harris, Anne M. Archibald, António H. Ribeiro, Fabian Pedregosa, Paul van Mulbregt, and SciPy 1.0 Contributors. SciPy 1.0: Fundamental Algorithms for Scientific Computing in Python. *Nature Methods*, 17:261–272, 2020.

[30] Rand R. Wilcox. *Robust Measures of Location*, pages 129–145. Springer New York, New York, NY, 2010.

[31] Hadley Wickham. *ggplot2: Elegant Graphics for Data Analysis*. Springer-Verlag New York, 2016.

[32] Zuguang Gu, Lei Gu, Roland Eils, Matthias Schlesner, and Benedikt Brors. circlize implements and enhances circular visualization in r. *Bioinformatics*, 30(19):2811–2812, 06 2014.

[33] Shuangbin Xu, Meijun Chen, Tingze Feng, Li Zhan, Lang Zhou, and Guangchuang Yu. Use ggbreak to effectively utilize plotting space to deal with large datasets and outliers. *Frontiers in Genetics*, 12:774846, 2021.

[34] David Hugh-Jones. *ggmagnify: Create a Magnified Inset of Part of a "Ggplot" Object*, 2024. R package version 0.4.1.9000, <https://hughjonesd.github.io/ggmagnify/>.

## A The lm-quant-toolkit overview

The lm-quant-toolkit is a suite of tools to facilitate large neural network quantization research. It includes a quantization harness tool to drive quantization experiments on large language models and vision models, to collect and summarize experiment data for further analysis. It also includes tool to prepare experiment meta data and visualization tools to interpret experiment results. Specifically, lm-quant-toolkit consists of:

- LLM quantization harness tool

- Kurtosis Metrics Measuring Tool
- Sensitivity Score Measuring Tool
- Calibration Dataset Generation Tool

Most tools are implemented in Python and are extensively tested under the Python 3.11.9. The visualization tools are implemented in R. The usage of these tools is elaborated in the following sections.

The Python tools depend on Python libraries such as transformers, datasets, numpy, PyTorch, among others. A few Python libraries are patched to support the proposed quantization methods. Specifically, required patched dependencies include AutoGPTQ (for CUDA 12.5 compatibility), HQQ (support SensiBoost/KurtBoost extension), lm\_eval (for end-to-end LLM performance evaluation), clip\_benchmark (for vision model evaluation). These dependencies are installed automatically as part of setup process.

The visualization tools facilitate visualizing the experiment results, the weight distribution, and generating insights of the latent features to quantize LLMs more efficiently. Most visualization tools are implemented in R and leverage the open-source plot libraries such as ggplot2 [31], circlize [32], ggbreak [33], and ggmagnify [34].

To setup the test harness and visualization tools, follow the instructions on <https://github.com/schnell18/lm-quant-toolkit.git>.

### A.1 Kurtosis Metrics Measuring Tool

This tool calculates the Kurtosis metrics of weight matrices layer-by-layer inside a particular large language model. The Kurtosis metrics are crucial to identify sensitive layers to improve the accuracy of quantization. This tool accepts a list of Hugging Face-compliant model identifiers. The output of this tool is a series of .csv files under specified directory. Each file contains the Kurtosis metrics for corresponding models.

The tool is implemented in Python and provides a convenient CLI interface to enable shell scripting. It is included in the `dump.py` file under the `src` folder in the `lm-quant-toolkit` project.

### A.2 Sensitivity Score Measuring Tool

This tool calculates the sensitivity scores of each layer of a particular large language model. The sensitivity scores are crucial to identify sensitive layers to improve the accuracy of quantization. This tool accepts a list of Hugging Face-compliant model identifiers. The output of this tool is a series of .csv files, each containing the sensitivity score for corresponding model. These files are crucial inputs to guide the SensiBoost and Sensitivity-based MiLP.

The tool is implemented in Python and provides a convenient CLI interface to enable shell scripting. It is compatible with any transformer-based LLMs with an implementation of the popular Hugging Face transformers library. It is located separately in the `dump.py` file under the `src` folder in the `lm-quant-toolkit` project, which helps to reduce unnecessary dependencies. A typical usage is demonstrated in the code snippet as follows:

The code snippet demonstrates how to calculate the sensitivity scores for a series of Qwen2.5 models using 4 calibration datasets under 12 bit budgets.

### A.3 Calibration Dataset Generation Tool

This tool generates a small synthesized dataset named Branch of Science (denoted as BoS, published on Hugging Face), which includes a few hundred of textual definitions for science, art and business topics such as Mathematics, Physics, Chemistry, Law, Music and Journalism, among others. The dataset is intended to validate whether the sensitivity property generalizes to diverse datasets.

The tool generates an initial dataset in .csv format which requires further processing. The output of this tool is random due to the generative nature of LLM. This tool requires a Llama-2-7B model being served with an OpenAI compatible RESTful API endpoint. User can either use a hosted API endpoint or deploy a local instance by following the instruction at the end of this section.